2021 NDIA Ground Vehicle Systems Engineering and Technology Symposium
Power and Mobility Technical Session
August 10-12, Novi, Michigan

SOH-based Battery Reconfiguration for Improved Energy Efficiency and Mission Extension of Battery Systems

Le Yi Wang[1], George Yin[2], Yi Ding[3]
[1]Department of Electrical and Computer Engineering, Wayne State University
[2]Department of Mathematics, University of Connecticut
[3]US Army CCDC Ground Vehicle Systems Center

Abstract

This paper analyzes the system-level state of health (SOH) and its dependence on the SOHs of the battery modules within the battery system. Due to the stochastic nature of battery aging processes and their dependance on charge/discharge, depth, temperature, and environment conditions, prior or long-term prediction of each module's SOH is difficult. Based on estimated SOHs of battery modules during battery operation, we demonstrate how the SOH of the entire system decays when battery modules age and become increasingly diversified in their maximum ampere-hour capacities. System-level energy efficiency is analyzed. It is shown that by using battery reconfiguration after a length of service, the overall battery usable capacities can be utilized more efficiently, leading to extended operational ranges of the battery system. Analysis methods and simulation studies are presented.

I. Introduction

New generations of military ground vehicles depend increasingly on battery systems in powering their movements, equipment, and operations. Consequently, reliability, efficiency, and health of battery systems are of critical importance for military operations. Due to unpredictable chemical processes, dependance on charge/discharge rate and depth, temperature, and environment conditions, the aging processes of battery modules are stochastic and difficult to predict, either prior to their deployment or over a long horizon during operation. While passenger cars experience loss of battery capacities over time, military vehicles encounter far more harsh environmental conditions, demand faster charging time, and endure deeper discharge depth for sustained operating ranges. All these factors impose more stress on battery modules and imply faster and more uneven aging processes than civil applications. As a result, to ensure endurance of battery systems in their military deployment, it is critically important that battery systems remain operational even with reduced and increasingly uneven battery capacities.

[0]This research was supported in part by the Army Research Office under Grant W911NF-19-1-0176.

This paper analyzes the system-level state of health (SOH) and its relationship to the SOHs of its battery modules. Typical large-scale battery systems in ground vehicles consist of battery modules that are interconnected by serial connection to increase voltage and parallel connection to increase ampere-hour (Ah) capacity. Such networking structures introduce a physical relationship between battery modules' SOHs and the SOH of the entire battery system. Battery aging processes are random and depend significantly on charge/discharge rate and depth and their operational environment conditions. When SOHs of battery modules decay, the SOH of the entire system is reduced accordingly.

Battery aging has been extensively studied at cell levels, including their basic mechanism [1], SOH estimation [2], cycle depths that affect aging processes [3], and temperature effects [4]. Battery aging models have been introduced to facilitate real-time SOH prediction [5]. The typical features of the aging process have been observed as slow aging first, followed by accelerated loss of capacity, then rapid aging after a certain knee point [6], [7]. Typical battery aging models have been proposed [8], [9]. In our recent work, data-based aging analysis [10], online SOH estimation [11], and SOH-based charging process [12] have been investigated.

This paper starts with a description of the battery systems in consideration in Section II. Section III presents an analysis of system-level battery efficiency. Under uneven battery capacities, we introduce the notation of total usable energy, maximum operational energy, and energy efficiency. By taking into consideration of uneven states of charge (SOC) of battery modules, the energy efficiency is further reduced. Section IV investigates the impact of battery aging on the system-level SOH. Battery regrouping methods and optimal strategies are introduced in Section V. The efficiency improvement by regrouping is proposed and its impact examined. The battery regrouping methods are evaluated by using case studies in Section VI. Finally, some closing remarks are given in Section VII.

II. Battery Systems

The illustrative scheme of the battery system studied in this paper is shown in Fig. 1. To facilitate a clarified study on the main issues, we impose some simplifications on battery modules.

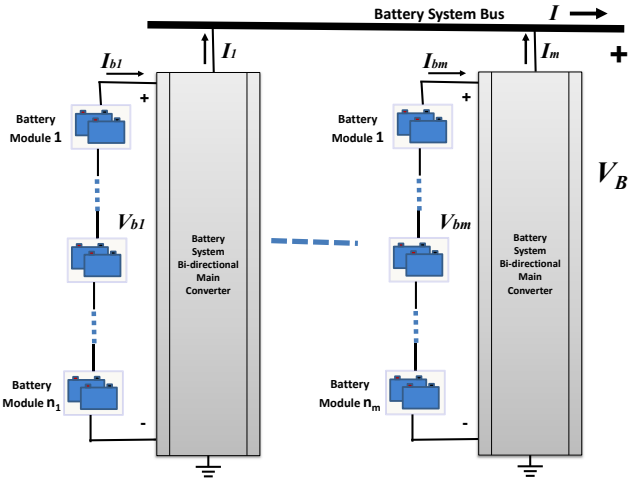

Fig. 1. System structure of a battery system.

1) In this paper, we consider n battery modules that are grouped into m strings. Each string has n_i modules, $i = 1, \ldots, m$, with $n = \sum_{i=1}^{m} n_i$. Suppose that when they are new, the battery modules have nearly uniform rated maximum capacity $Q_{\max}$. We do not distinguish variations of the actual capacities between charge and discharge, ignore dependence of the capacity on the temperature, charge/discharge rate, and omit its change as a function of the battery SOC.
Since we focus on SOH analysis, it is assumed that all battery modules have rated voltage V_b. The n_i modules in the ith string are serially connected whose terminal voltage V_{bi} is then converted to the rated bus voltage V_B of the battery system via a bi-directional DC-DC converter. The converter also serves as the controller for charge/discharge current I_{bi}. The m DC-DC converters allow flexible grouping of battery modules with variable numbers in each string.
The power loss of the convertors is ignored. Consequently, the bus-side current I_i and the string-side current I_{bi} are related by

$$I_{bi} = \frac{V_B}{V_{bi}} I_i, i = 1, \ldots, m,$$

and the total battery current I is

$$I = \sum_{i=1}^{m} I_i = \sum_{i=1}^{m} \frac{V_{bi}}{V_B} I_{bi}.$$

2) Within the ith string, there are n_i modules. For clarity of analysis, we first ignore the small deviations in open-circuit voltage (OCV) of the battery modules and assume the uniform OCV V_{oc} for all modules. As a result,

$$V_{bi} = n_i V_{oc},$$

which implies that

$$I = \frac{V_{oc}}{V_B} \sum_{i=1}^{m} n_i I_{bi}.$$

III. System-Level Capacity Efficiency

A. Capacity Efficiency

Consider the ith string that consists of n_i modules. In our analysis that involves the SOC limits on charge/discharge processes, we use the *permitted SOC* of a battery module as its operational range that will be labeled as $[S_{\min}, S_{\max}]$.[1]

[1]The permitted SOC range is smaller than a battery's chemical SOC range and is often determined by the terminal voltage limits of the battery protection circuits that safeguard the battery from over-charging and over-discharging. It is a common practice to normalize the range so that $S_{\min} = 0$ and $S_{\max} = 1$.

Let the SOCs of the battery modules at time t of a discharge operation be denoted by

$$S(t) = \begin{bmatrix} S_1(t) \\ \vdots \\ S_{n_i}(t) \end{bmatrix}.$$

We shall first consider an ideal scenario in which one starts with a uniformly and fully charged string, namely $S(0) = [1, \ldots, 1]^T$. The negative impact of disparity in the initial SOCs will be shown later.

Suppose that after k charge/discharge cycles, the battery modules' capacities Q_j^i (Ah), $j = 1, \ldots, n_i$, are ordered by their current capacities

$$Q_1^i(k) \le Q_2^i(k) \le \cdots \le Q_{n_i}^i(k).$$

We emphasize that due to randomness and uneven aging processes, this ordering changes with k.

If the battery system is discharged at a constant rate $I = I_0$ (A), since $Q_1^i = Q_{\min}^i$ is the smallest capacity of the string, the discharge must stop when Module 1 reaches $S_{\min}$, resulting in the maximum discharge time for the whole string as

$$T^i = \frac{Q_1^i(S_{\max} - S_{\min})}{I_0} \quad \text{(hour)}.$$

It follows that

$$S(T^i) = \begin{bmatrix} S_{\min} \\ S_{\max} - (S_{\max} - S_{\min})Q_1^i/Q_2^i \\ \vdots \\ S_{\max} - (S_{\max} - S_{\min})Q_1^i/Q_{n_i}^i \end{bmatrix}.$$

Consequently, the total discharged energy is

$$n_i V_{oc} I_0 T^i = n_i V_{oc}(S_{\max} - S_{\min})Q_1^i \quad \text{Wh}. \quad (1)$$

On the other hand, the total usable energy, if all stored electricity in the modules is fully utilized, is

$$\sum_{j=1}^{n_i} Q_j^i (S_{\max} - S_{\min}) V_{oc}.$$

The system-level energy efficiency η_i of this string is defined as

$$\begin{aligned} \eta_i &= \frac{n_i V_{oc}(S_{\max} - S_{\min})Q_1^i}{\sum_{j=1}^{n_i} Q_j^i (S_{\max} - S_{\min}) V_{oc}} \\ &= \frac{n_i Q_1^i}{\sum_{j=1}^{n_i} Q_j^i} \\ &= \frac{Q_{\min}^i}{\overline{Q^i}} \end{aligned}$$

where $Q_{\min}^i = Q_1^i$ is the minimum capacity and $\overline{Q^i} = \frac{1}{n_i}\sum_{j=1}^{n_i} Q_j^i$ is the average capacity.

Example 3.1: For an illustration, consider a battery system of 16 modules, that are divided into 4 strings with 4 modules in each string. All modules have the same rated terminal voltage 12 (V) and maximum capacity $Q = 50$ (Ah) when they are new. The battery system terminal rated voltage is 48 (V) and system-level rated capacity 200 (Ah). This amounts to a battery system of rated energy capacity 9.6 (KWh) when it is new. For safety, the SOC range is limited to $[0.3, 0.85]$, namely $S_{\min} = 0.3$ and $S_{\max} = 0.85$.

Suppose that after battery aging, the 16 modules have randomly reduced and more diverse capacities. Table I lists capacity values and the energy efficiencies of the strings.

TABLE I
BATTERY CAPACITIES (AH) AFTER DEGRADATION AND MAXIMUM ENERGY EFFICIENCY

String	Q_1	Q_2	Q_3	Q_4	$Q_{\min}$	$\overline{Q}$	η
1	46	38	49	40	38	43.25	0.879
2	40.2	45.5	47.1	44.2	40.2	44.25	0.908
3	35.8	43.2	39.7	46.9	35.8	41.4	0.865
4	37.5	38.6	43.5	47.3	37.5	41.725	0.899

B. Impact of SOC Management on Energy Efficiency

During battery operation, the SOCs of the battery modules become unequal. This SOC disparity reduces energy efficiency. To quantify this impact, suppose that at the starting time $t = 0$ of discharge the SOCs are

$$S(0) = \begin{bmatrix} S_1(0) \\ \vdots \\ S_{n_i}(0) \end{bmatrix}.$$

The maximum discharge time for the jth module, if operated alone, is

$$T_j^i = \frac{Q_j^i(S_j(0) - S_{\min})}{I_0}.$$

Since discharge must stop when one module reaches its lower limit, the string discharge time is

$$\begin{aligned} T^i &= \min_{j=1,\ldots,n_i} T_j^i \\ &= \frac{1}{I_0} \min_{j=1,\ldots,n_i} Q_j^i (S_j(0) - S_{\min}) \\ &\le \frac{1}{I_0}(S_{\max} - S_{\min})Q_{\min}^i. \end{aligned}$$

It follows that the total discharged energy is reduced from (1) to

$$n_i V_{oc} I_0 T^i = n_i V_{oc} \min_{j=1,\dots,n_i} Q_j^i (S_j(0) - S_{\min}) \quad (2)$$

and the energy efficiency is reduced to

$$\begin{aligned} &\frac{n_i V_{oc} \min_{j=1,\dots,n_i} Q_j^i (S_j(0) - S_{\min})}{\sum_{j=1}^{n_i} Q_j^i (S_{\max} - S_{\min}) V_{oc}} \\ &= \frac{\min_{j=1,\dots,n_i} Q_j^i (S_j(0) - S_{\min})}{(S_{\max} - S_{\min})\overline{Q^i}} \\ &\le \eta_i. \end{aligned}$$

It is noted that the worst-case scenario is when the minimum-capacity module has the lowest SOC, namely,

$$\arg \min_{j=1,\dots,n_i} Q_j^i = \arg \min_{j=1,\dots,n_i} S_j(0).$$

When this scenario occurs, the lowest energy efficiency happens as

$$\frac{Q_{\min}^i (\min_{j=1,\dots,n_i} S_j(0) - S_{min})}{(S_{\max} - S_{\min})\overline{Q^i}}.$$

Example 3.2: Impact of SOC imbalance on energy efficiency can be numerically demonstrated by using the data in Example 3.1. We will use the first string as an example. For this string, $Q_{\min} = 38$ and $\overline{Q} = 42.2$.

Suppose that for this string, there are 10% random variations of $S(0)$ below $S_{\max} = 0.85$. we assign randomly such SOC deviations to the four battery modules in Table II. These values result in

$$\begin{aligned} &\min_{j=1,\dots,4} Q_j (S_j(0) - S_{\min}) = 19.874, \\ &(S_{\max} - S_{\min})\overline{Q^i} = 23.79, \end{aligned}$$

which reduces the string energy efficiency from 90% to 83.5%.

TABLE II
SOC IMBALANCE ON MAXIMUM ENERGY EFFICIENCY

Module	1	2	3	4	η
Q	46	38	49	40	
$S(0) = S_{\max}$	0.85	0.85	0.85	0.85	0.900
Random $S(0)$	0.788	0.823	0.806	0.799	0.835

IV. BATTERY AGING AND SYSTEM-LEVEL SOH

When battery systems are new, it is possible to select modules that are relatively uniform in their capacities in a string. However, during battery operation, the capacities will decrease in highly variable rate. Most common aging features of battery cells are depicted in Fig. 2, see [2], [3], [5], [9], [10] for detail. The Ah throughput ratio T is defined as the total charge/discharge ampere hours divided by the rated maximum capacity of a battery cell within the designated SOC range. In other words, T is the equivalent number of full-range charge/discharge cycles from $S = S_{\min}$ to $S_{\max}$.

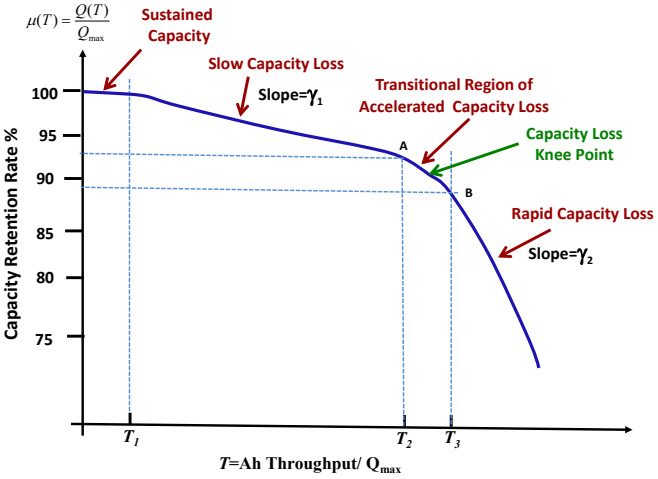

Fig. 2. Typical capacity reduction of lithium-ion batteries.

Battery aging is characterized by the loss of usable capacity, as the ratio $\mu(T) = Q(T)/Q_{\max}$, namely the current usable capacity to the rated maximum capacity when it is new. The typical battery aging curve in Fig. 2 is characterized by several key parameters. For $T \in [0, T_1]$ a relatively new battery maintains its capacity. From $T = T_1$ to T_2, the battery shows slow aging that can be modeled by a nearly constant (negative) slope γ_1. Then the battery aging accelerates in a relatively small interval $[T_2, T_3]$, reducing its values from $\mu(T_2) = A$ to $\mu(T_3) = B$. The middle point $(T_2 + T_3)/2$ is called the *knee point*. After T_3, the battery experiences rapid capacity loss with aggregated rate γ_2. Individual aging features of battery modules in a string are random and define collectively the SOH dynamics of the system-level SOH. Consequently, when modules lose capacity gradually, the total energy efficiency of the string, and then the entire battery system, will be affected.

For each battery module, under a given parameter set $\theta = [T_1, T_2, T_3, A, B, \gamma_1, \gamma_2]$, the function $\mu(T)$ in Fig. 2 may be represented by the following mathematics model:

$$\mu(T) = \begin{cases} 1, & 0 \le T \le T_1 \\ 1 - \gamma_1(T - T_1), & T_1 < T \le T_2 \\ A, & T = T_2 \\ g(T), & T_2 < T < T_3 \\ B, & T = T_3 \\ B - \gamma_2(T - T_3), & T > T_3 \end{cases} \tag{3}$$

For the function $\mu(T)$ to be continuous, $A = 1 - \gamma_1(T_2 - T_1)$. In this paper, the function $g(T)$ is a spline fitting, satisfying the boundary conditions

$$g(T_2) = A, \quad g(T_3) = B. \tag{4}$$

V. Battery Regrouping

Under the simplification assumption of uniform open-circuit voltages, identical $S_{\min}$ and $S_{\max}$, and equal distribution of the current to strings, the total usable energy of the entire battery system is

$$E_{\text{total}} = \sum_{i=1}^{m} \sum_{j=1}^{n_i} Q_j^i (S_{\max} - S_{\min}) V_{oc}.$$

On the other hand, the total used energy when starting from uniform $S_{\max}$ is

$$E_{\text{used}} = \sum_{i=1}^{m} n_i V_{oc} (S_{\max} - S_{\min}) Q_{\min}^i.$$

It follows that the energy efficiency for the entire battery system under these idealized conditions is

$$\eta = \frac{\sum_{i=1}^{m} n_i Q_{\min}^i}{\sum_{i=1}^{m} \sum_{j=1}^{n_i} Q_j^i}. \tag{5}$$

In the special case that n and m are fixed with $n/m = k$ which is an integer, and each string has the same number $n_i = k$ of battery modules, the energy efficiency (5) is simplified to

$$\eta = \frac{E_{\text{used}}}{E_{\text{total}}} = \frac{\frac{1}{m} \sum_{i=1}^{m} Q_{\min}^i}{\frac{1}{n} \sum_{i=1}^{m} \sum_{j=1}^{n_i} Q_j^i}. \tag{6}$$

The energy efficiency (5) depends critically on how the battery modules are grouped. We now introduce a basic regrouping algorithm by sorting battery modules on the basis of their capacity values at a given point of cycle life T.

Battery Regrouping Algorithm:

1) Initial Condition: $H_1(T) = \{Q_1(T), \ldots, Q_n(T)\}$.
2) Iterative Grouping: For $i = 1, \ldots, m$,
   a) select $G_i(T)$ to be the set of k modules of the smallest Q values in $H_i(T)$.
   b) $H_{i+1}(T) = H_i(T) \ominus G_i(T)$.

The following theorem shows the optimality of the grouping algorithm of battery modules.

Theorem 5.1: Suppose that n and m are fixed, $n/m = k$ is an integer, and each string has the same number k of battery modules. Then the Battery Grouping Algorithm is optimal in the sense of achieving the highest energy efficiency.

Proof: This is proved by induction. T is omitted from notation. Suppose that for a given H_i, E_i^{opt} is the optimal energy that can be used by grouping within H_i. Note that E_i^{opt} is monotone non-increasing if one battery module in H_i is replaced by a module of smaller capacity.

Now, suppose that from the given H_i, G_i is selected by the Battery Grouping Algorithm. Then $H_i = H_{i+1} \oplus G_i$ such that for any $Q_a \in H_{i+1}$ and any $Q_b \in G_i$, we have $Q_a \ge Q_b$. Suppose we exchange one $Q_a \in H_{i+1}$ and $Q_b \in G_i$ with $Q_a > Q_b$. By monotonicity, the optimal used energy of the new H_{i+1} will not increase. Also, since

$$Q_a > Q_b \ge \min_{Q_k \in G_i} Q_k,$$

the used energy for the new G_i cannot increase. Since this is valid for all i, by induction, the Battery Grouping Algorithm is optimal. □

This theorem indicates that it is useful to group the battery modules after their capacities degrade with large variations.

Example 5.1: We now use the data in Example 3.1 to show the benefits of regrouping.

Suppose that for the group of battery modules in Table I, we now apply the Battery Grouping Algorithm. The resulting new strings and the string energy efficiencies are shown in Table III.

TABLE III
IMPROVEMENT OF MAXIMUM ENERGY EFFICIENCY BY REGROUPING

String	Q_1	Q_2	Q_3	Q_4	$Q_{\min}$	$\overline{Q}$	η
1	35.8	37.5	38	38.6	35.8	37.475	0.955
2	39.7	40	40.2	43.2	39.7	40.775	0.974
3	43.5	44.2	45.5	46	43.5	44.8	0.971
4	46.9	47.1	47.3	49	46.9	47.575	0.986

To compare the total energy efficiency, if we do not perform re-grouping, then from Table I,

$$\frac{1}{4}\sum_{i=1}^{4} Q^i_{\min} = 37.875,$$
$$\frac{1}{16}\sum_{i=1}^{4}\sum_{j=1}^{4} Q^i_j = 42.656,$$

which has the total energy efficiency 88.8%.

In contrast, if we perform the Battery Regrouping Algorithm, the data in Table III shows that

$$\frac{1}{4}\sum_{i=1}^{4} Q^i_{\min} = 41.475,$$
$$\frac{1}{16}\sum_{i=1}^{4}\sum_{j=1}^{4} Q^i_j = 42.656,$$

which has the total energy efficiency 97.2%.

Discussions on Hardware Realization

Battery regrouping can be achieved by manually re-assigning battery modules to different strings as a maintenance procedure, or by designing electric switches to reconnect battery modules without moving them physically, or by employing suitable power electronic circuits that can change networking structures of battery modules. Fig. 3 illustrates a conceptual scheme for such a reconfiguration system.

In this scheme, illustrated with four strings, each battery module can be freely assigned to any string. If it is assigned to String 1, then all other strings will be automatically disconnected from this module. Since group reorganization occurs only periodically over a relatively long time, such switches may offer simplicity, low cost, and low power loss.

VI. AN ILLUSTRATIVE CASE STUDY

In this section, we employ a basic setup to illustrate the main issues and methods of this paper. The battery

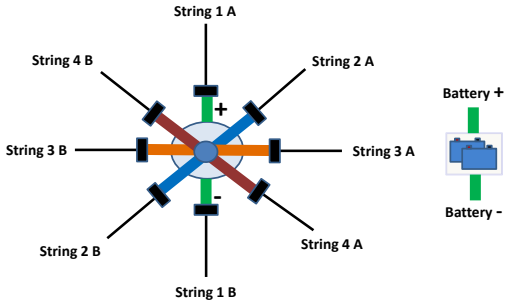

Fig. 3. A functional scheme for battery module reconfiguration.

system consists of $n = 100$ modules, with rated voltage 24 (V) and rated new maximum capacity $Q = 100$ (Ah). The modules are grouped into four ($m = 4$) strings of 25 modules each ($n_1 = n_2 = n_3 = n_4 = 25$). As a result, the battery terminal rated voltage is 600 (V) and system-level rated capacity 400 (Ah). This amounts to a battery system of energy capacity 240 (KWh) when it is new. A 1C charge for the entire battery system is 400 (A), but is equally distributed to be 100 (A) for each string.

Each battery module has an unknown aging characteristic parameter set

$$\theta = [T_1, T_2, T_3, A, B, \gamma_1, \gamma_2]$$

depicted in Fig. 2. For this study, the ranges of the parameters are shown in Table IV.

TABLE IV
PARAMETER RANGES

Parameter	Range
T_1	$300 \sim 500$
T_2	$2500 \sim 3500$
A	$1 - \gamma_1(T_2 - T_1)$
$T_3 - T_2$	$200 \sim 300$
B	$A - B = 0.02 \sim 0.03$
γ_1	$0.5 \sim 3 \times 10^{-5}$
γ_2	$1 \sim 5 \times 10^{-4}$

Since battery aging processes are stochastic, we assume that such processes are independent and identically distributed. Prior to simulation, for each battery module, its parameter set is selected randomly and independently. The parameter set is then fixed without further alternation in simulation.

The initial capacity values are all equal to the rated capacity 100 (Ah). The aging curves are derived by

using linear interpolation with

$$g(T) = A - \frac{A-B}{T_3 - T_2}(T - T_2).$$

Fig. 4 demonstrates a sample of 100 aging curves generated randomly by our simulation program.

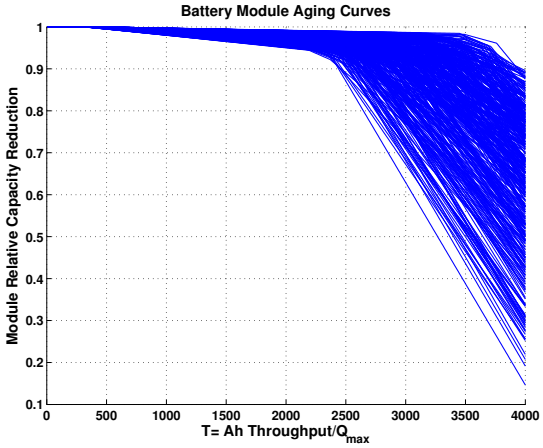

Fig. 4. Randomly generated 100 battery aging curves for this case study.

We start with the scenario of battery operation without regrouping. The 100 battery modules with random aging characteristics are grouped into four strings of 25 modules each. Without any regrouping, the top plot of Fig. 5 shows the maximum energy efficiency of the strings. Since the energy efficiency of a string is highly dependent of capacity variations within the string, over time when battery aging takes effect, the efficiency becomes substantially reduced. This leads to substantial loss of energy efficiency for the entire battery system, illustrated in the bottom plot of Fig. 5.

On the other hand, if we apply the Battery Regrouping Algorithm, the energy efficiency of the entire battery system can be significantly improved. Fig. 6 compares energy efficiency trajectories of three scenarios: no grouping, regrouping every $T = 1000$, and regrouping every $T = 500$. Efficiency improvement at $T = 4000$ is $\eta = 0.4581$ without regrouping; $\eta = 0.6857$ when regrouping is applied at every $T = 1000$ interval; $\eta = 0.7748$ when regrouping is applied at every $T = 500$.

In terms of the total available energy (Wh) after T equivalent life cycles, Fig. 7 demonstrates how much the usable energy is lost under different grouping strategies. Similarly, Fig. 8 shows how much the accumulative usable battery energy is unused due to battery

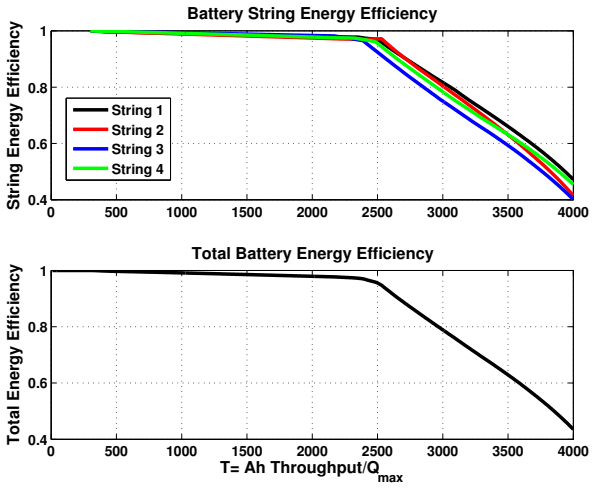

Fig. 5. Energy efficiency trajectories of the four strings and the entire battery system. Top Plot: The energy efficiencies of the four strings. Bottom Plot: The energy efficiency of the entire battery system

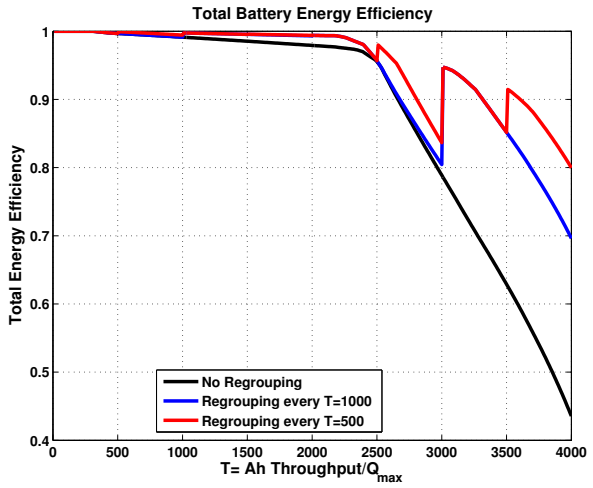

Fig. 6. Energy efficiency improvements of the entire battery system by using regrouping at different intervals.

grouping issues. Over the total $T = 4000$ equivalent life cycles, the total usable battery electricity amounts to 3.5550 (MWh). Without battery re-grouping, the actual used energy is only 3.1935 (MWh), a loss of battery energy capacity 0.3615 (MWh). In comparison, if the battery system is regrouped every $T = 1000$, 3.4015 (MWh) is realized with a much lower loss of 0.1535 (MWh). Further improvement is shown with regrouping every $T = 500$, with 3.4258 (MWh) realized energy and a further loss reduction to 0.1292 (MWh).

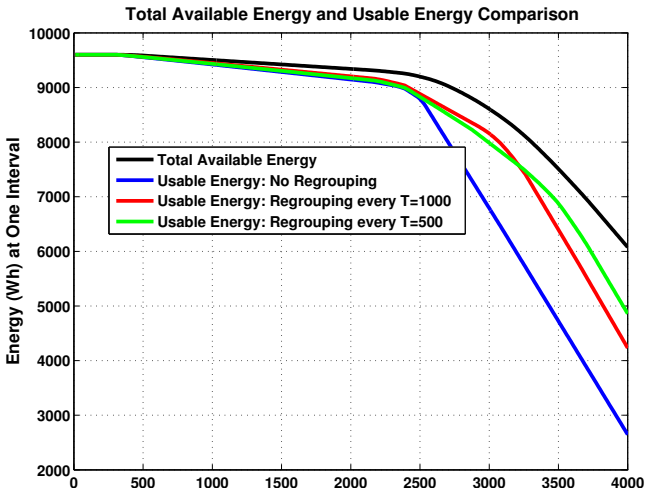

Fig. 7. Comparison the total available energy (Wh) of the battery system after T operating range with the actually usable energy due to different strategies of battery grouping.

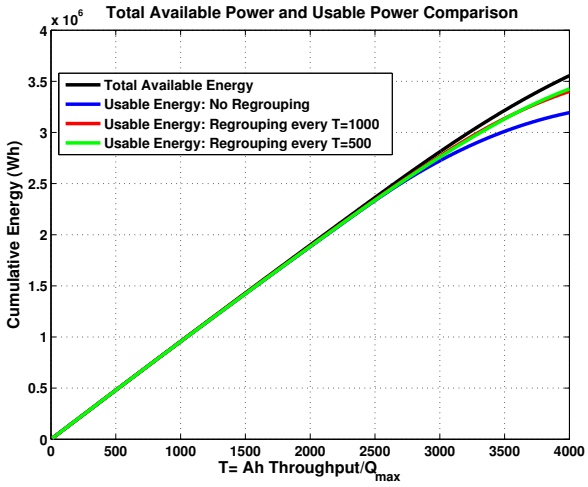

Fig. 8. Comparison the total cumulative available energy (Wh) of the battery system within $T = 4000$ with the actually usable cumulative energy due to different strategies of battery grouping.

VII. Concluding Remarks

This paper introduces the notion of battery energy efficiency that captures the impact of uneven battery capacities on the system-level energy usage and the lost capacity. Our analysis establishes a relationship between individual battery modules' aging processes and the system-level SOH, and indicates potential remedies for improving energy efficiency of the entire battery system. Some simple conceptual hardware systems for realizing battery regrouping are proposed, that can be implemented by either physical switches or power electronic circuits. Further studies are planned to combine real-time SOH estimation, SOC estimation, and the regrouping process, and to develop comprehensive control methods to further improve battery system efficiency and durability.

References

[1] Y. Gao, J. Jiang, C. Zhang, W. Zhang and Y. Jiang, "Aging Mechanisms Under Different State-Of-Charge Ranges and the Multi-Indicators System of State-Of-Health for Lithium-Ion Battery with Li(NiMnCo)O2 Cathode," J Power Sources, 400, 641-651 (2018).

[2] A. Barré, B. Deguilhem, S. Grolleau, M. Gérard, F. Suardand D. Riu, "A Review On Lithium-Ion Battery Ageing Mechanisms and Estimations for Automotive Applications," J Power Sources, 241, 680-689 (2013).

[3] X. Han, L. Lu, Y. Zheng, X. Feng, Z. Li, J. Liand M. Ouyang, "A Review On the Key Issues of the Lithium Ion Battery Degradation Among the Whole Life Cycle," eTransportation, 1, 100005 (2019).

[4] K. Jalkanen, J. Karppinen, L. Skogström, T. Laurila, M. Nisulaand K. Vuorilehto, "Cycle Aging of Commercial NMC/graphite Pouch Cells at Different Temperatures," Appl Energ, 154, 160-172 (2015).

[5] E. Sarasketa-Zabala, I. Gandiaga, E. Martinez-Laserna, L.M. Rodriguez-Martinezand I. Villarreal, "Cycle Ageing Analysis of a LiFePO4/graphite Cell with Dynamic Model Validations: Towards Realistic Lifetime Predictions," J Power Sources, 275, 573-587 (2015).

[6] W. Diao, S. Saxenaand M. Pecht, "Accelerated Cycle Life Testing and Capacity Degradation Modeling of LiCoO2-graphite Cells," J Power Sources, 435, 226830 (2019).

[7] I. Bloom, B.W. Cole, J.J. Sohn, S.A. Jones, E.G. Polzin, V.S. Battaglia, G.L. Henriksen, C. Motloch, R. Richardson, T. Unkelhaeuser, D. Ingersolland H.L. Case, "An Accelerated Calendar and Cycle Life Study of Li-ion Cells," J Power Sources, 101, 238-247 (2001).

[8] Y. Lee, H. Choi, C. Ha, J. Yu, M. Hwang, C. Dohand J. Choi, "Cycle Life Modeling and the Capacity Fading Mechanisms in a graphite/LiNi0.6Co0.2Mn0.2O2 Cell," J Appl Electrochem, 45, 419-426 (2015).

[9] J. Schmalstieg, S. Käbitz, M. Eckerand D.U. Sauer, "A Holistic Aging Model for Li(NiMnCo)O2 Based 18650 Lithium-Ion Batteries," J Power Sources, 257, 325-334 (2014).

[10] Xinyu Jia, Caiping Zhang, Le Yi Wang, Linjing Zhang, Weige Zhang, The Degradation Characteristics and Mechanism of Li[Ni0.5Co0.2Mn0.3]O2 Batteries at Different Temperatures and Discharge Current Rates, Journal of The Electrochemical Society, 2019.

[11] Jichao Hong, Zhenpo Wang, Wen Chen, Leyi Wang, Peng Lin, Changhui Qu, Online Accurate State of Health Estimation for Battery Systems on Real-World Electric Vehicles with Variable Driving Conditions Considered, *Journal of Cleaner Production*, accepted in 2021.

[12] Xue Li, Jiuchun Jiang, Le Yi Wang, Dafen Chen, Yanru Zhang, Caiping Zhang, A capacity model based on charging process for state of health estimation of lithium ion batteries, *Applied Energy*, 177, pp. 537-543, 2016.